THE JOURNAL OF BIOLOGICAL CHEMISTRY VOL. 290, NO. 35, pp. 21292–21304, August 28, 2015

The Positively Charged COOH-terminal Glycosaminoglycan-binding CXCL9(74–103) Peptide Inhibits CXCL8-induced Neutrophil Extravasation and Monosodium Urate Crystal-induced Gout in Mice*

Received for publication, March 4, 2015, and in revised form, June 25, 2015 Published, JBC Papers in Press, July 16, 2015, DOI 10.1074/jbc.M115.649855

Vincent Vanheule[‡], Rik Janssens[‡], Daiane Boff[§], Nikola Kitic[¶], Nele Berghmans[‡], Isabelle Ronsse[‡], Andreas J. Kungl[¶], Flavio Almeida Amaral[§], Mauro Martins Teixeira[§], Jo Van Damme[‡], Paul Proost[‡1,2], and Anneleen Mortier[‡1,3]

From the [‡]Laboratory of Molecular Immunology, Department of Microbiology and Immunology, Rega Institute, KU Leuven, 3000 Leuven, Belgium, the [§]Departamento de Fisiologia e Biofisica, Instituto de Ciencias Biologicas, Universidade Federal de Minas Gerais, Belo Horizonte, Minas Gerais 31270-901, Brazil, and the [¶]Department of Pharmaceutical Chemistry, Institute of Pharmaceutical Sciences, Karl-Franzes Universität, 8010 Graz, Austria

Background: Chemokines, such as CXCL8 and CXCL9, drive leukocyte migration to an inflammation site.
Results: CXCL9(74–103), derived from CXCL9, lacks leukocyte-attracting activity but competes with CXCL8 for GAG binding and inhibits neutrophil migration in two murine acute inflammation models.
Conclusion: Through inhibition of chemokine-GAG interaction, CXCL9(74–103) blocks neutrophil migration.
Significance: CXCL9(74–103) may be a lead molecule for development of anti-inflammatory agents.

The ELR⁻CXC chemokine CXCL9 is characterized by a long, highly positively charged COOH-terminal region, absent in most other chemokines. Several natural leukocyte- and fibroblast-derived COOH-terminally truncated CXCL9 forms missing up to 30 amino acids were identified. To investigate the role of the COOH-terminal region of CXCL9, several COOH-terminal peptides were chemically synthesized. These peptides display high affinity for glycosaminoglycans (GAGs) and compete with functional intact chemokines for GAG binding, the longest peptide (CXCL9(74–103)) being the most potent. The COOH-terminal peptide CXCL9(74–103) does not signal through or act as an antagonist for CXCR3, the G protein-coupled CXCL9 receptor, and does not influence neutrophil chemotactic activity of CXCL8 *in vitro*. Based on the GAG binding data, an anti-inflammatory role for CXCL9(74–103) was further evidenced *in vivo*. Simultaneous intravenous injection of CXCL9(74–103) with CXCL8 injection in the joint diminished CXCL8-induced neutrophil extravasation. Analogously, monosodium urate crystal-induced neutrophil migration to the tibiofemural articulation, a murine model of gout, is highly reduced by intravenous injection of CXCL9(74–103). These data show that chemokine-derived peptides with high affinity for GAGs may be used as anti-inflammatory peptides; by competing with active chemokines for binding and immobilization on GAGs, these peptides may lower chemokine presentation on the endothelium and disrupt the generation of a chemokine gradient, thereby preventing a chemokine from properly performing its chemotactic function. The CXCL9 peptide may serve as a lead molecule for further development of inhibitors of inflammation based on interference with chemokine-GAG interactions.

Chemokines constitute a group of small structurally related chemotactic proteins indispensable for the coordination of leukocyte migration during inflammation (1). In addition, they are essential factors in the control of leukocyte mobilization from primary or secondary lymphoid organs, in the generation of lymphoid follicles, and in the homing of leukocytes to specific organs and tissues (1). Upon tissue injury, sterile inflammation, or infection, chemokines are locally produced by tissue cells and resident leukocytes. Through their G protein-coupled receptors, which are expressed by specific leukocytes, chemokines induce the endothelial adhesion of leukocyte subtypes followed by their extravasation and directional migration toward the site of infection (2, 3). In addition to receptor binding, a major role in chemokine activity has been allocated to interactions with glycosaminoglycans (GAGs),[4] such as heparin, heparan sulfate (HS), and dermatan sulfate (DS) (4, 5). This interaction occurs between sulfated domains of GAGs and

* This research was supported by the Interuniversity Attraction Poles Programme initiated by the Belgian Science Policy Office (I.A.P. Project 7/40), the Fund for Scientific Research of Flanders (FWO-Vlaanderen Projects G.0764.14, G.0773.13, and G.0D66.13), the Brazilian National Council for Scientific and Technological Development (CNPq), and the Concerted Research Actions of the Regional Government of Flanders (GOA/12/017). The Hercules foundation of the Flemish government provided funding to purchase LC-MS/MS equipment (Contract AKUL/11/31). The authors declare that they have no conflicts of interest with the contents of this article.

[1] Both authors contributed equally to this work.
[2] To whom correspondence should be addressed: Laboratory of Molecular Immunology, Rega Institute, KU Leuven, Minderbroedersstraat 10, 3000 Leuven, Belgium. Tel.: 32-16-337347; Fax: 32-16-337340; E-mail: paul.proost@rega.kuleuven.be.
[3] Recipient of a postdoctoral research grant from FWO-Vlaanderen.

[4] The abbreviations used are: GAG, glycosaminoglycan; HS, heparan sulfate; DS, dermatan sulfate; MSU, monosodium urate; PBMC, peripheral blood mononuclear cell; RP, reversed-phase; TAMRA, tetramethylrhodamine; LMWH, low molecular weight heparin.

basic amino acid motifs of chemokines. The GAG binding motif on chemokines frequently takes the form *X*BB*X*B*X* or *X*BBB*XX*B*X*, in which B represents a basic and *X* represents any non-basic amino acid (6). In general, these GAG binding motifs are located at a site distant from the specific receptor-binding domain, often within the COOH-terminal region of the molecule. Although chemokine-GAG binding largely depends on electrostatic interactions, a certain degree of specificity has been ascribed to this interaction, suggested to be due to van der Waals and hydrogen bond forces (5, 7).

Chemokine binding to GAGs has been proven to be indispensable for chemokine activity *in vivo* (8–16). Abrogated GAG binding (tested using chemokine variants with mutations in their GAG binding motif) results in abrogated activity *in vivo*, although receptor binding and chemotactic activity *in vitro* are seldom affected (9–11). In addition, reduced chemokine-induced leukocyte migration is seen in mice with disturbed HS synthesis (8, 13, 14).

Based on *in vitro* data, this role for GAG binding in chemokine functioning *in vivo* can be explained by its importance in chemokine gradient formation, cis- or trans- (on endothelial cells) presentation of chemokines, chemokine transcytosis across venular endothelial cells, and stabilization of oligomer formation and protection against enzymatic degradation (1, 8, 9, 11, 17–20). More recently, *in vivo*, chemokines were shown to localize within capillary venules in a GAG-dependent way (13, 18). Moreover, in zebrafish, fluorescently labeled CXCL8 was found to form an extracellular gradient in tissue that decays within a distance of 50–100 μm from the producing cells and was immobilized on the local venous vasculature (12). Both gradient formation and immobilization were dependent on extracellular HS proteoglycans. Analogously, endogenous HS-dependent gradients of CCL21 were detected within mouse skin (21). In all of the above cases, destruction of these gradients abolished directional leukocyte migration. Indeed, these data support the hypothesis that chemokine production at sites of inflammation results in the generation of GAG-mediated chemokine gradients in the extracellular matrix and presentation by the GAGs on the endothelial cell wall, thereby preventing their diffusion and degradation and retaining high local concentration of the produced chemokines (22). These chemokine gradients continuously drive the adhesion, extravasation, and tissue infiltration of specific leukocyte subsets.

Chemokine activity goes far beyond the mere induction of leukocyte migration. Chemokines have also been shown to be key players in embryonic development and angiogenesis, the formation of new blood vessels from pre-existing ones, both in embryonic (physiological) and adult (pathological) conditions (23, 24). ELR$^+$CXC chemokines, such as CXCL6 and CXCL8, clearly show angiogenic properties, whereas ELR$^-$CXC chemokines, including CXCL4/PF4 (platelet factor 4) and CXCL9, are angiostatic molecules. Based on their impact on leukocyte infiltration and angiogenesis, a role in tumor biology is conceivable (25, 26). Fine-tuning chemokine activity is critical to control inflammation in time, space, and intensity (27). Besides other regulatory mechanisms, such as tightly regulated gene expression and the presence of atypical receptors, post-translational modification undeniably controls chemokine activity and thereby leukocyte accumulation and inflammation (28–32). Specific and limited processing of chemokines (truncation, glycosylation, or citrullination), executed by enzymes that are co-expressed under inflammatory conditions, can alter their biological activity due to increased or decreased receptor binding/signaling, changed receptor specificity, or altered GAG binding affinity (28). By up- or down-regulating chemokine activity, these enzymes determine the shape and speed of the immune response, triggering rapid leukocyte mobilization upon infection, but also efficiently dampening inflammation upon resolution of infection.

The secreted ELR$^-$CXC chemokine CXCL9/Mig (monokine induced by interferon-γ) consists of 103 amino acids and attracts activated T lymphocytes, preferentially of the Th1 phenotype, and NK cells through activation of the CXC chemokine receptor 3 (CXCR3) (33). Like the other CXCR3 ligands CXCL10 and CXCL11, the production of CXCL9 is induced by the Th1 cytokine interferon (IFN)-γ. In contrast to CXCL10 and CXCL11 and to almost all other chemokines, the COOH-terminal region of CXCL9 is remarkably long and basic with 50% positively charged amino acids. Although these CXCR3 ligands show a high degree of redundancy *in vitro*, this apparent redundancy seems to be absent *in vivo* (34). This is probably due to differential temporal and spatial expression patterns and different binding characteristics toward their shared receptors.

This study aims to obtain more insight into the contribution of this unique COOH-terminal region of CXCL9. We have explored the possible role of the COOH-terminal region by chemically synthesizing COOH-terminal CXCL9 peptides. We show that a COOH-terminal CXCL9 peptide, cleaved from natural CXCL9, competes with CXCL8 for GAG binding and inhibits CXCL8-induced neutrophil extravasation *in vivo*. Moreover, this peptide was able to neutralize neutrophil influx into the joint in monosodium urate (MSU) crystal-induced gout, a model for human gout in mice.

Experimental Procedures

Cells—Human peripheral blood mononuclear cells (PBMCs) and neutrophils were isolated from fresh human buffy coats as described previously (35, 36). CXCL9 production was induced on PBMCs (5×10^6 cells/ml in RPMI 1640 with 2% (v/v) fetal calf serum (FCS)) with 10 μg/ml double-stranded RNA (dsRNA) (poly(rI:rC); Sigma-Aldrich) and 20 ng/ml IFN-γ (PeproTech, Rocky Hill, NJ) for 20–120 h at 37 °C (35, 36). Confluent human diploid skin muscle-derived fibroblasts were stimulated in Eagle's minimal essential medium containing 2% (v/v) FCS with 10 μg/ml dsRNA, 20 ng/ml IFN-γ, and 5 μg/ml lipopolysaccharide (LPS; Difco) for 96 h at 37 °C. Chinese hamster ovary (CHO) cells, transfected with human CXCR3A (CHO/CXCR3A), CXCR3B (CHO/CXCR3B), and CXCR4 (CHO/CXCR4), were a gift from M. Parmentier (Université Libre de Bruxelles, Brussels, Belgium) and cultured as described (37).

Purification and Identification of CXCL9 Isoforms from PBMC- and Fibroblast-conditioned Medium—Natural human CXCL9 was purified to homogeneity in a four-step purification procedure (38). Briefly, CXCL9 was detected by an enzyme-linked immunosorbent assay (ELISA) and purified by adsorp-

tion to controlled pore glass and heparin-Sepharose affinity chromatography. The eluted material was desalted through dialysis with a 6.5 kDa cut-off membrane before Mono S cation exchange (GE Healthcare) chromatography. Final separation was performed by reversed-phase high performance liquid chromatography (RP-HPLC) on a 2.1 × 220-mm Brownlee C8 Aquapore RP-300 column (PerkinElmer Life Sciences). Of the RP-HPLC effluent, 0.7% was split on-line to an ion trap mass spectrometer (Bruker Daltonics, Bremen, Germany). Profile spectra were collected, averaged within the UV absorption (λ = 214 nm) peaks containing CXCL9 immunoreactivity, and deconvoluted to determine the average relative molecular mass (M_r). This M_r was compared with the theoretical average M_r of intact or truncated CXCL9. In addition, the NH_2-terminal sequence of the isolated CXCL9 forms was determined by Edman degradation (Procise 491 cLC sequencer, Applied Biosystems, Foster City, CA).

Chemical Synthesis of the COOH-terminal CXCL9 Peptides—COOH-terminal CXCL4 and CXCL9 peptides (*i.e.* CXCL4(47–70), CXCL9(74–103), CXCL9(79–103), CXCL9(82–103), CXCL9(86–103), and CXCL9(1–78)) and CXCL8 were chemically synthesized based on Fmoc (*N*-(9-fluorenyl)methoxycarbonyl) chemistry using an Activo-P11 automated solid phase peptide synthesizer (Activotec, Cambridge, UK), as described by Loos *et al.* (38). Part of the CXCL4(47–70), CXCL9(74–103), and CXCL8 material was site-specifically biotinylated at the NH_2 terminus using biotin-*p*-nitrophenyl ester (Novabiochem, Darmstadt, Germany) as described recently (37, 39). Synthetic peptides were purified on a Source 5-RPC column (4.6 × 150 mm; GE Healthcare) and eluted in an acetonitrile gradient in 0.1% (v/v) trifluoroacetic acid (TFA). A portion (0.7%) of the column effluent was split for analysis by online ion trap mass spectrometry. Fractions containing homogenous CXCL9 peptide were pooled, lyophilized, and dissolved in ultrapure water (MilliQ; Merck Millipore, Billerica, MA). CXCL9(1–78) protein was folded as described previously (38). Multiple tests were applied to determine the protein concentrations and purity (*i.e.* bicinchoninic acid (BCA) protein assay (Pierce), SDS-PAGE, and NH_2-terminal sequencing based on Edman degradation).

Isothermal Fluorescence Titration—To study the interaction between CXCL9(74–103) and GAGs and CXCL8, titration experiments were performed as described by Gerlza *et al.* (40), using TAMRA-labeled synthetic CXCL9(74–103), HS (Iduron BN1), low molecular weight heparin (LMWH; Iduron BN5), DS (Iduron BN1), and recombinant CXCL8 (ProtAffin Biotechnologie AG, Graz, Austria).

Calcium Mobilization by CXCL9 Peptides through CXCR3—The capacity of the CXCL9 peptides to induce signaling through human CXCR3, resulting in an increase of the intracellular Ca^{2+} concentration or desensitization toward CXCL9 stimulation, was tested on CXCR3-transfected CHO cells, as described previously (41). In the case of preincubation, CXCL9 was incubated with CXCL9(74–103) for 10 min prior to the addition to cells.

Binding of CXCL9(74–103) to Cellular GAGs and Competition with CXCL8—Binding of biotinylated CXCL9(74–103) to CHO/CXCR3A, CHO/CXCR3B, and CHO/CXCR4 cells was assessed by flow cytometric analysis. To inhibit the sulfation of cellular GAGs, CHO cells were cultured in the presence of 100 mM sodium chlorate ($NaClO_3$). After 24 h, cells were detached with phosphate-buffered saline (PBS) enriched with 0.02% (w/v) EDTA for 5–10 min at 37 °C, washed with culture medium, and resuspended after 1 h in ice-cold assay buffer (PBS + 2% (v/v) FCS). Subsequently, cells (3×10^5) were labeled with biotinylated CXCL9(74–103) at different dilutions for 30 min on ice. After washing, cells were incubated with streptavidin-allophycocyanin (BD Biosciences) for 30 min on ice in the dark. Finally, cells were washed three times with ice-cold assay buffer and analyzed using a FACSCalibur flow cytometer (BD Biosciences). In parallel, to confirm inhibition of sulfation of cellular GAGs, part of the cells were stained with a mouse monoclonal anti-human HS antibody (Immunosource, Schilde, Belgium), washed with assay buffer, incubated with a secondary phycoerythrin-labeled goat anti-mouse antibody (BD Biosciences), and analyzed by flow cytometry. Statistical analyses were performed using the Mann-Whitney *U* test. Analogously, binding of 300 nM biotinylated CXCL8 in the presence or absence of CXCL9(74–103) was compared on CHO/CXCR4 cells.

Competition of the COOH-terminal CXCL9 Peptides for Chemokine Binding to GAG-coated Plates—The ability of the COOH-terminal CXCL9 peptides to compete for GAG binding with the inflammatory chemokines CXCL8, CXCL11, or CCL2 was evaluated on GAG binding plates (BD Biosciences), which adsorb GAGs without modification to retain the protein-binding characteristics. Heparin (25 μg/ml; Iduron, Manchester, UK) or HS (25 μg/ml; Iduron), diluted in standard assay buffer (100 mM NaCl, 50 mM sodium acetate, 0.2% (v/v) Tween 20, pH 7.2) were coated overnight at room temperature on the plasma-polymerized surface of GAG binding plates. After three wash steps with standard assay buffer, the plates were blocked with blocking buffer (standard assay buffer enriched with 0.2% (w/v) gelatin) for 1 h at 37 °C. Blocking buffer was discarded, and dilutions of CXCL9 peptide combined with recombinant human CXCL8(1–77) (PeproTech), recombinant human CXCL11(1–73) (PeproTech), or recombinant biotinylated CCL2(1–76) (ProtAffin Biotechnologie AG) (in blocking buffer) were added in duplicate and incubated for 2 h at 37 °C. Unbound peptide and chemokine were removed by three washes with standard assay buffer. Bound CXCL8 or CXCL11 was incubated with biotinylated polyclonal rabbit anti-human CXCL8 or CXCL11 (PeproTech), diluted in blocking buffer, followed by detection with horseradish peroxidase-labeled streptavidin. Bound biotinylated CCL2 was directly detected using streptavidin-HRP (40). Subsequently, the plates were washed, the peroxidase activity was quantified by adding a horseradish peroxidase substrate solution, and conversion of 3,3′,5,5′-tetramethylbenzidine supplemented with 0.004% (v/v) H_2O_2 was measured at 450 nm using a spectrophotometer. Percentage inhibition of chemokine binding to GAG was calculated as follows.

$$\text{Percentage inhibition} = \frac{\text{OD}(x\ \text{nM chemokine} + y\ \text{nM CXCL9 peptide}) - \text{OD}(\text{control sample})}{\text{OD}(x\ \text{nM chemokine}) - \text{OD}(\text{control sample})} \times 100 \quad \text{(Eq. 1)}$$

Statistical analyses (comparison with the corresponding excess of CXCL9(74–103)) were performed using the Mann-Whitney *U* test.

ELISA-like Assay for Hetero-oligomerization of CXCL9(74–103) with CXCL8—Hetero-oligomerization of CXCL9 peptide with CXCL8 was quantified on high protein binding ELISA plates (Corning Inc., Tewksbury, MA). In brief, 1 μg/ml or 500 ng/ml human recombinant CXCL8(1–77) (PeproTech) diluted in PBS was coated overnight at 4 °C on 96-well plates. Plates were washed three times with assay buffer (0.5% (v/v) Tween 20 in PBS) and blocked at 37 °C with assay buffer enriched with 0.1% (w/v) casein. Subsequently, a dilution series of biotinylated CXCL9 peptide was added and allowed to interact with CXCL8. After washing, biotinylated CXCL9 peptide was detected by peroxidase-conjugated streptavidin. Peroxidase activity was quantified by measuring the conversion of 3,3′,5,5′-tetramethylbenzidine at 450 nm.

Neutrophil Migration in Vitro and in Vivo—The chemotactic activity of CXCL8(6–77) in combination with CXCL9 peptides for neutrophilic granulocytes *in vitro* was compared using a 48-well Boyden chamber-based chemotaxis assay, and migrated neutrophils were counted microscopically, as described previously (42). *In vivo* blood vessel extravasation of circulating neutrophil granulocytes to the knee cavity was examined by injection of endotoxin-free recombinant CXCL8(1–77) (PeproTech) or vehicle (10 μl of 0.9% NaCl) in the tibiofemural articulation of C57Bl/6 mice. A group of mice received intravenously CXCL9 peptide (100 μg; 100 μl) at the same time as CXCL8 or saline. Endotoxin concentrations were evaluated with the *Limulus* amoebocyte lysate test (Cambrex, East Rutherford, NJ). For preparation of MSU crystals, 1.68 mg of uric acid was dissolved in 500 ml of a 0.01 M NaOH solution heated to 70 °C. The pH of the solution was kept between pH 7.1 and 7.2. Once dissolved, the solution was filtered through a sterile syringe filter with a 0.22-μm pore size. The sterile solution was stirred for 24 h at room temperature to form the crystals, the supernatant was discarded, and the MSU crystals were washed with ethanol. Subsequently the size of the crystals was reduced by sonication, dried, and resuspended in PBS. PBS or 100 μg of crystals (in 10 μl) were injected in the tibiofemoral knee joint. A group of mice received intravenous CXCL9 peptide (10, 30, or 100 μg in 100 μl) or vehicle. The cells present in the tibiofemoral articulation were harvested 3 h after CXCL8 or MSU crystal administration by washing the cavity with 10 μl of 3% (w/v) bovine serum albumin in PBS and diluted in 90 μl of 3% (w/v) bovine serum albumin in PBS. The number of total leukocytes was determined by counting leukocytes in a Neubauer chamber after staining with Turk's solution. Differential counts were obtained from cytospin preparations by evaluating the percentage of each leukocyte type on a slide stained with May-Grunwald-Giemsa. Percentages of cells present in the joint lavages were statistically compared between CXCL9 peptide-treated and untreated mice using the Mann-Whitney *U* test. The experimental *in vivo* protocols (involving the use of laboratory animals) were reviewed and approved by the Animal Ethical Committee of KU Leuven or the University of Minas Gerais, and Belgian and European guidelines concerning the handling of laboratory animals were followed. Mice were sacrificed by injection of an overdose of Nembutal prior to the collection of joint lavages.

Results

Purification and Identification of Natural COOH-terminally Truncated CXCL9—Previously, induction experiments showed that high amounts of CXCL9 were produced by PBMCs and fibroblasts upon stimulation with IFN-γ and dsRNA (35). Furthermore, in the case of fibroblasts, synergistic induction of CXCL9 was observed when fibroblasts were stimulated with IFN-γ and dsRNA or LPS, resulting in massive (~1 μg/10^6 cells) secretion of CXCL9. In contrast, in the case of PBMCs, LPS clearly inhibited IFN-γ-induced CXCL9 production. In order to investigate posttranslational modifications on CXCL9, natural CXCL9 was purified from the conditioned medium of PBMCs stimulated with dsRNA and IFN-γ and from fibroblasts stimulated with dsRNA, IFN-γ, and LPS. Secreted proteins were separated, combining heparin affinity, cation exchange and RP chromatography. Analysis by mass spectrometry of those fractions containing CXCL9, as determined by ELISA, showed that these fractions did not contain any intact CXCL9; however, several COOH-terminally truncated isoforms were present (*i.e.* CXCL9(1–74), CXCL9(1–75), CXCL9(1–76), CXCL9(1–77), CXCL9(1–78), CXCL9(1–81), CXCL9(1–82), CXCL9(1–84), and CXCL9(1–85)) (Table 1). Interestingly, all of these CXCL9 isoforms lost their characteristic cationic COOH-terminal region. To illustrate, Fig. 1 shows a RP-HPLC profile of specific CXCL9-containing fractions selected after heparin affinity and cation exchange chromatographic purification of the conditioned medium from PBMCs stimulated with dsRNA and IFN-γ. ELISA data revealed the presence of CXCL9 in RP-HPLC fractions 49–53. More detailed analysis of the proteins present in these fractions by mass spectrometry disclosed the presence of two different proteins with a relative M_r of 9019.40 and 8718.35, which correspond to the theoretical relative molecular masses of CXCL9(1–81) and CXCL9(1–78), respectively.

Chemical Synthesis of COOH-terminal CXCL9 Peptides—Whether the highly cationic COOH-terminal peptides fulfill a biological function on their own was investigated. Therefore, the CXCL9 COOH-terminal peptides CXCL9(74–103), CXCL9(79–103), CXCL9(82–103), and CXCL9(86–103) were chemically synthesized and purified by RP-HPLC, and their M_r was confirmed by ion trap mass spectrometry (Table 1). In addition, COOH-terminally cleaved CXCL9(1–78) was synthesized, folded, and purified.

Interaction of CXCL9(74–103) with Soluble GAGs—Given the high number of positive charges (more than 1 in 2 amino acids), one could presume a GAG binding function for the COOH-terminal region of CXCL9. Therefore, the affinity of the longest of the synthesized peptides (*i.e.* CXCL9(74–103)) for LMWH, HS, and DS was determined by isothermal fluorescence titration (Fig. 2). Using this technique, TAMRA fluorescence quenching was measured upon interaction of NH_2-terminally TAMRA-labeled CXCL9(74–103) with LMWH, HS, or DS. The resulting binding isotherms were analyzed by nonlinear regression according to a bimolecular association reaction (43), which gave K_d values of 61.21, 4.76, and 4.38 nM, respec-

TABLE 1

Overview of the CXCL9 isoforms that were purified from the conditioned medium of PBMCs and fibroblasts and of the complementary COOH-terminal CXCL9 peptides synthesized to investigate their potential anti-inflammatory function

For clarity, basic amino acids were underlined, and amino acids 11–59 were left out of the amino acid sequences.

	CXCL9 isoform	Amino Acid Sequence	Mr (theor.)	Purified from
	1-103	$_{1}$TPVVRKGRCS$_{10\cdots60}$VKELIKKWEKQVSQKKKQKNGKKHQKKKVLKVRKSQRSRQKKTT$_{103}$	11720.7	/
Purified from conditioned medium	1-85	$_{1}$TPVVRKGRCS$_{10\cdots60}$VKELIKKWEKQVSQKKKQKNGKKHQK$_{85}$	9539.0	PBMCs
	1-84	$_{1}$TPVVRKGRCS$_{10\cdots60}$VKELIKKWEKQVSQKKKQKNGKKHQ$_{84}$	9410.9	PBMCs
	1-82	$_{1}$TPVVRKGRCS$_{10\cdots60}$VKELIKKWEKQVSQKKKQKNGKK$_{82}$	9145.6	PBMCs
	1-81	$_{1}$TPVVRKGRCS$_{10\cdots60}$VKELIKKWEKQVSQKKKQKNGK$_{81}$	9017.4	PBMCs/Fibroblasts
	1-78	$_{1}$TPVVRKGRCS$_{10\cdots60}$VKELIKKWEKQVSQKKKQK$_{78}$	8718.1	PBMCs
	1-77	$_{1}$TPVVRKGRCS$_{10\cdots60}$VKELIKKWEKQVSQKKKQ$_{77}$	8589.9	Fibroblasts
	1-76	$_{1}$TPVVRKGRCS$_{10\cdots60}$VKELIKKWEKQVSQKKK$_{76}$	8461.8	Fibroblasts
	1-75	$_{1}$TPVVRKGRCS$_{10\cdots60}$VKELIKKWEKQVSQKK$_{75}$	8333.6	Fibroblasts
	1-74	$_{1}$TPVVRKGRCS$_{10\cdots60}$VKELIKKWEKQVSQK$_{74}$	8205.5	Fibroblasts
Synthesized	86-103	$_{86}$KKVLKVRKSQRSRQKKTT$_{103}$	2199.7	/
	82-103	$_{82}$KHQKKKVLKVRKSQRSRQKKTT$_{103}$	2721.3	/
	79-103	$_{79}$NGKKHQKKKVLKVRKSQRSRQKKTT$_{103}$	3020.6	/
	74-103	$_{74}$KKKQKNGKKHQKKKVLKVRKSQRSRQKKTT$_{103}$	3661.4	/

tively. Interestingly, CXCL9(74–103) shows 12-fold higher affinity for HS compared with LMWH. It can be concluded that CXCL9(74–103) binds with high but different affinity to these glycosaminoglycans.

CXCL9(74–103) Interacts with Cellular GAGs—To confirm these results on cellular GAGs, CXCL9(74–103) was also site-specifically biotinylated at the NH_2 terminus (to avoid modification of the lysine side chains and interference of biotin groups with GAG binding), and binding of biotinylated CXCL9(74–103) to CHO cells was evaluated by flow cytometric analysis (Fig. 3). As reported, CXCL9(74–103) is not able to bind to CXCR3 (44). Therefore, CHO/CXCR3A and CHO/CXCR3B cells were used to evaluate the binding of CXCL9(74–103) to GAGs. As an additional control, a cell type with an irrelevant receptor for CXCL9 and the peptide, namely CHO/CXCR4 cells, was used. Flow cytometric analysis demonstrated that CXCL9(74–103) binds dose-dependently to CXCR3A, CXCR3B, and CXCR4/CHO cells (Fig. 3*B*). Because CXCL4 is known to be one of the strongest GAG binding chemokines (37, 45), we also evaluated the interaction of an NH_2-terminally biotinylated COOH-terminal peptide of CXCL4, namely CXCL4(47–70), with cellular GAGs as a reference peptide. Fig. 3*B* shows that CXCL4(47–70) binds dose-dependently to GAGs on CXCR3A, CXCR3B, and CXCR4/CHO cells but with lower affinity than CXCL9(74–103). To ensure that binding was GAG-mediated, CHO cells were treated with $NaClO_3$ to reduce the expression of HS. $NaClO_3$ treatment significantly reduced the expression of HS on the CHO cells (on average 75%) and consequently the binding of CXCL9(74–103) and CXCL4(47–70) (Fig. 3*A*).

COOH-terminal CXCL9 Peptides Compete with CXCL8, CXCL11, and CCL2 for Binding to Heparin, HS, or Cellular GAGs—The main human neutrophil attractant, CXCL8, has been demonstrated to be a relatively strong heparin-binding molecule (46). Using GAG binding plates in an ELISA-like assay, the ability of CXCL9(74–103) to inhibit binding of CXCL8 to heparin was evaluated (Fig. 4*A*). As expected, given its highly positively charged nature, CXCL9(74–103) clearly competed with CXCL8. If the molar concentration of CXCL9(74–103) exceeded the concentration of CXCL8 by a factor 10, CXCL8 binding to heparin was reduced by 50%. Interestingly, the shorter COOH-terminal CXCL9 peptides CXCL9(79–103), CXCL9(82–103), and CXCL9(86–103) were less potent competitors. To achieve a 50% reduction of CXCL8 binding, a 100-fold (at least) excess of the shorter CXCL9 peptides was needed. Interestingly, CXCL9(74–103) competed with CXCL8 for heparin binding with a similar potency as intact CXCL9(1–103). Additionally, the capacity of CXCL9(1–78) to compete for GAG binding was evaluated. A 10-fold molar excess of CXCL9(1–78) did not inhibit the binding of CXCL8 to heparin, suggesting that this CXCL9 isoform lost most of its capacity to bind to GAGs. GAG binding competition between CXCL9(74–103) and CXCL8 was confirmed on CHO cells (Fig. 4*B*). Indeed, the binding of biotinylated CXCL8 to cellular GAGs was reduced by 50% in the presence of a 10-fold excess of CXCL9(74–103).

To evaluate whether GAG binding competition was restricted to the ELR^+CXC chemokine CXCL8, binding competition assays were also performed with the ELR^-CXC chemokine CXCL11, the most potent CXCR3 ligand, and the CC chemokine CCL2, a strong monocyte attractant (Fig. 4, *C* and *D*). CXCL9(74–103) clearly competed with both chemokines for GAG binding. Again, CXCL9(74–103) turned out to be the most potent CXCL9 COOH-terminal peptide. These results indicate that CXCL9(74–103) may compete with a broad range of chemokines belonging to different chemokine subfamilies.

CXCL9(74–103) and CXCL8 Do Not Oligomerize—Besides binding to GAGs and to their G protein-coupled receptors, chemokines tend to oligomerize (17). Both homophilic and het-

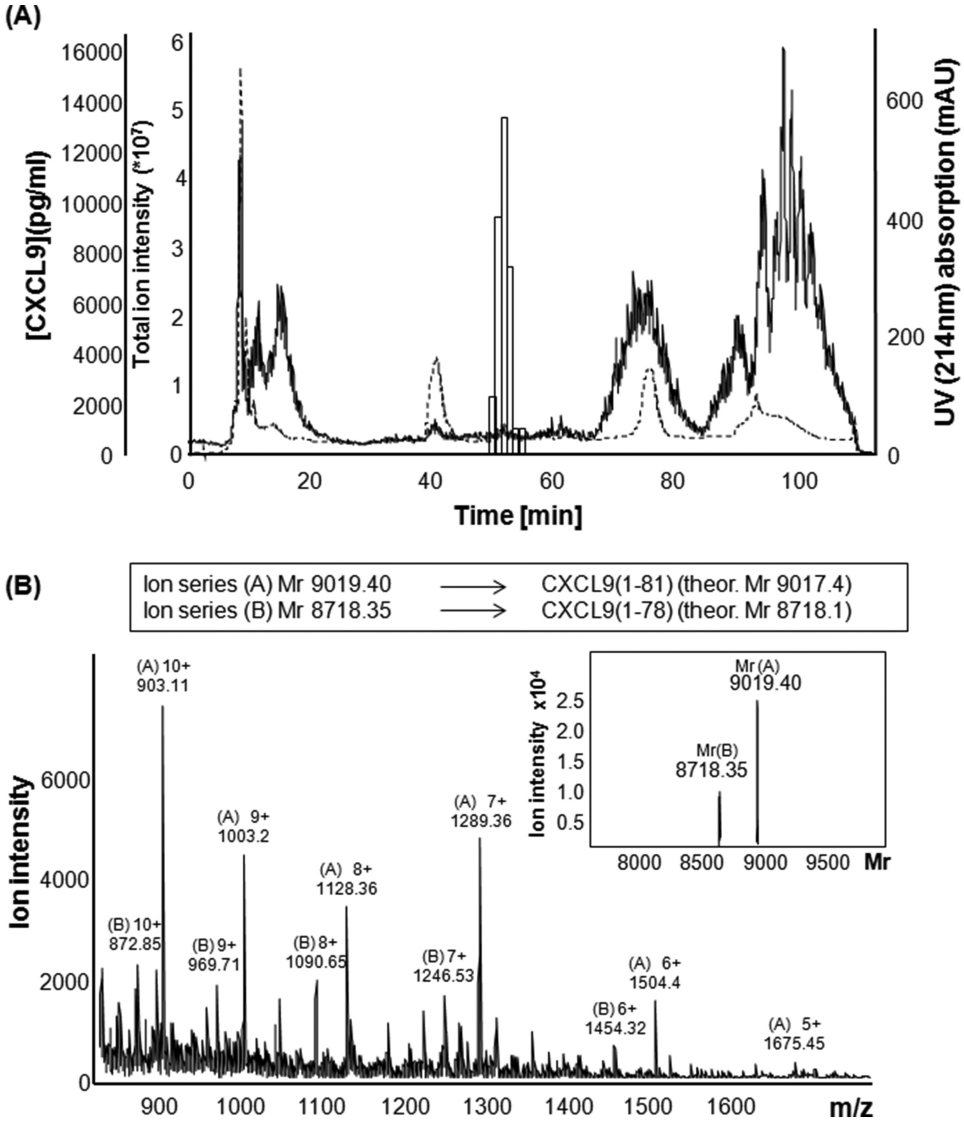

FIGURE 1. **Identification of COOH-terminally truncated isoforms of CXCL9 from leukocyte-derived conditioned medium.** PBMCs were stimulated with a combination of dsRNA and IFN-γ for 120 h. Conditioned medium was purified using a four-step chromatographic procedure. The results of the final C8 RP-HPLC separation are depicted in *A*. Proteins were eluted in an acetonitrile gradient in 0.1% (v/v) TFA and were detected on-line by UV absorption (λ = 214 nm) and by ion trap mass spectrometry. UV absorption (*dotted line*) and total ion chromatogram (representing the sum of all ions reaching the detector of the mass spectrometer; *solid line*) are shown in *A*. Subsequently, CXCL9 immunoreactivity of the RP-HPLC fractions was determined by ELISA (histograms; *A*). The mass spectra of CXCL9-positive fractions were more closely analyzed. *B*, averaged mass spectrum for molecules eluting in CXCL9-containing fractions 49–53, displaying the intensity of the detected ions with their specific mass/charge ratios. In order to calculate the relative molecular mass (M_r) of the proteins corresponding with these ions, Bruker deconvolution software was used (*inset* on the *right* in *B*). The experimentally determined M_r of the proteins is compared with the theoretical M_r of CXCL9 isoforms indicated in the *inset* at the *top* of *B*. *mAU*, milliabsorbance units.

erophilic interactions can be formed, and these interactions can dramatically affect a chemokine's biological activity. For example, CXCL8 and CXCL4 tend to dimerize, and this interaction decreases the potency of CXCL4 to inhibit proliferation of endothelial cells (47). This way, hetero-oligomerization might embody another degree of chemokine function regulation in a given *in vivo* chemokine environment. To exclude the possibility that CXCL9(74–103) reduces CXCL8 binding to GAGs through direct interaction with CXCL8, hetero-oligomerization of CXCL9(74–103) with CXCL8(1–77) was tested by isothermal fluorescence titration. When CXCL8 was titrated to the TAMRA-labeled CXCL9 peptide (600 nM), no significant interaction could be observed (Fig. 5). 10% quenching and late saturation of TAMRA fluorescence is indicative of a very weak and/or a rather nonspecific interaction between the two molecules. Analogously, no direct interaction between the peptide and CXCL8 was detected in an ELISA-like assay, in which the binding of biotinylated CXCL9(74–103) was measured on a 96-well plate coated with CXCL8 (data not shown). As a positive control, the COOH-terminal CXCL4 peptide (residues 47 to 70) and EGF were tested in parallel and displayed clear hetero-oligomerization, as reported recently (37).

CXCL9(74–103) No Longer Signals through CXCR3 and Does Not Influence in Vitro Chemotaxis of Neutrophils in Response to CXCL8—The longest of the synthesized CXCL9 peptides (*i.e.* CXCL9(74–103)) has been reported to be no longer able to bind to CXCR3, the cognate receptor for intact CXCL9

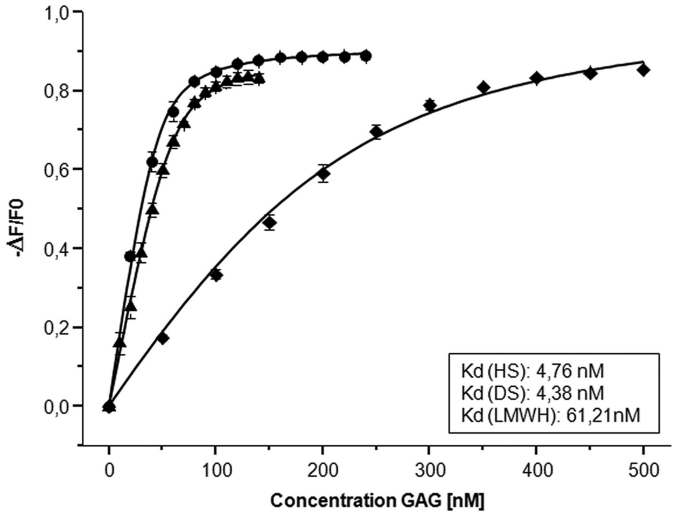

FIGURE 2. **Affinity of CXCL9(74–103) for GAGs as determined by isothermal fluorescence titration.** Interaction of TAMRA-CXCL9(74–103) and GAGs was determined by isothermal fluorescence titration. TAMRA fluorescence is dose-dependently quenched upon interaction with GAGs. LMWH (♦), HS (▲), and DS (●) binding isotherms of TAMRA-labeled CXCL9(74–103) (600 nM) are shown. The mean ± S.E. (*error bars*) ($n = 3$) relative change in fluorescence intensity following ligand addition is displayed: $\Delta F = F$ (fluorescence emission at a certain ligand concentration) $- F_0$ (fluorescence emission in the absence of ligand). K_d values were determined and included in the graph.

(CXCR3-B300-19 cells) (44). Analogously, we demonstrated that this peptide is unable to induce calcium-signaling in CXCR3-transfected CHO cells or to desensitize CXCR3 signaling to intact CXCL9 (Fig. 6*A*). Also, preincubation of CXCL9 with CXCL9(74–103) for 10 min did not influence the calcium-signaling capacity of intact CXCL9 (Fig. 6*B*). Thus, in contrast to intact CXCL9, CXCL9(74–103) no longer executes CXCR3-mediated functions.

To exclude any interference of CXCL9(74–103) with the interaction of CXCL8 with its receptor, the potency of CXCL9(74–103) to affect CXCL8-induced neutrophil migration *in vitro* in a Boyden chamber chemotaxis assay, assumed to be a GAG-independent process, was evaluated (Fig. 6*C*). Even at a dose of 300 ng/ml, CXCL9(74–103) did not influence the chemotactic potency of CXCL8 (1.5–15 ng/ml). No statistical differences on chemotactic responses were observed when neutrophils were stimulated with CXCL8 in the absence or presence of CXCL9 peptide. In addition, a cytotoxic effect of CXCL9(74–103) on neutrophils was excluded in a lactate dehydrogenase cytotoxicity assay (data not shown).

CXCL9(74–103) Lowers CXCL8- and MSU-induced Neutrophil Recruitment to the Joints—Based on its *in vitro* competition for GAG binding combined with its abrogated G protein-coupled receptor-dependent activity, CXCL9(74–103) might possess promising immunosuppressive properties. By competing with chemokines for GAG binding, this peptide might lower the chemokine's capacity to recruit leukocytes to a site of inflammation. Therefore, the potential anti-inflammatory capacity of CXCL9(74–103) was evaluated in two mouse models of acute inflammation (Fig. 7). Because CXCL8 is the main human neutrophil attractant and an abundant chemokine in the arthritic joint (48), CXCL8 was used as a prototypic inflammatory chemokine. In a first acute inflammation model, injection of 1 μg of CXCL8 into the tibiofemoral articulation of

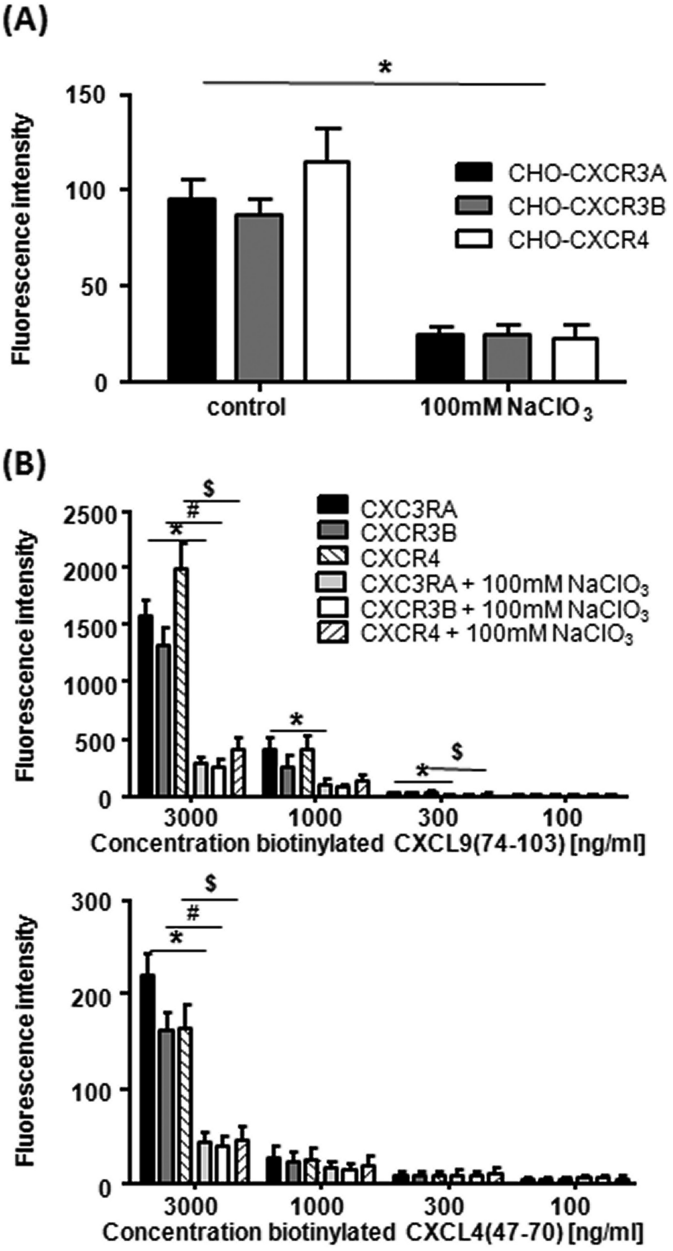

FIGURE 3. **Interaction of CXCL9(74–103) with GAGs on the cell membrane of CHO cells.** Binding of biotinylated CXCL9(74–103) and CXCL4(47–70) to CHO/CXCR3A, CHO/CXCR3B, and CHO/CXCR4 cells was assessed by flow cytometric analysis. To ensure that the binding was GAG-mediated, CHO cells were treated with sodium chlorate ($NaClO_3$) to reduce the expression of GAGs. *A*, expression of HS on CHO/CXCR3A, CHO/CXCR3B, and CHO/CXCR4 cells (untreated or treated with $NaClO_3$) as assessed by staining cells with a specific mouse monoclonal anti-human HS antibody and a secondary phycoerythrin-labeled goat anti-mouse antibody. *B*, dose-dependent binding of NH_2-terminally biotinylated peptides to CHO cells (untreated or treated with $NaClO_3$) as detected by streptavidin-allophycocyanin. A statistical comparison to evaluate the expression of HS (*A*) and the binding of biotinylated peptides (*B*) on cells treated or not treated with $NaClO_3$ was performed using the Mann-Whitney *U* test (*A*, *, $p < 0.05$; *B*, *, $p < 0.05$ for CXCR3A; #, $p < 0.05$ for CXCR3B; $, $p < 0.05$ for CXCR4).

C57BL/6 mice results in a massive influx of leukocytes (Fig. 7*A*). This massive influx into the knee cavity was clearly reduced upon concomitant intravenous injection of 100 μg of CXCL9(74–103) (a reduction from $\sim 43 \times 10^4$ cells to 14×10^4 cells). As shown by differential counting of the different leuko-

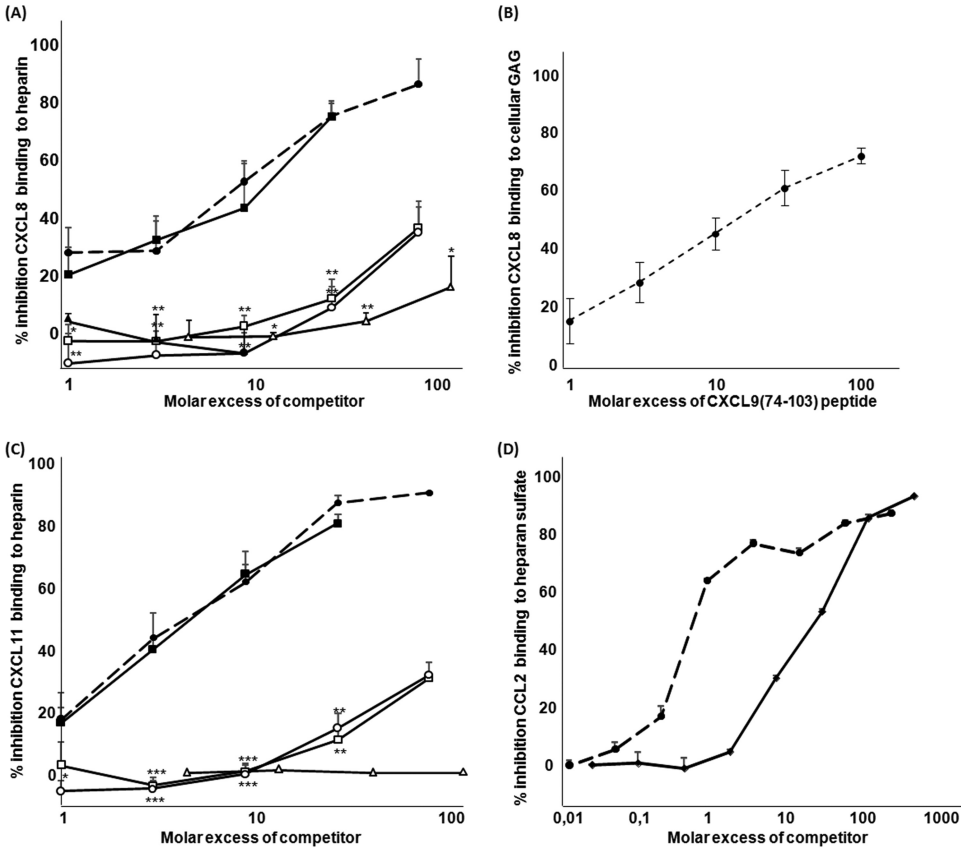

FIGURE 4. **COOH-terminal CXCL9 peptides compete with CXCL8, CXCL11 or CCL2 for binding to GAGs.** Competition between CXCL8 and COOH-terminal CXCL9 peptides for binding to heparin (*A*) and to CHO cells (*B*) was performed. *A*, CXCL8 (300, 100, 30, and 10 nM) was added to heparin (immobilized in 96-well plates) in the presence/absence of the indicated excess of competitor (CXCL9(74–103) (●), CXCL9(79–103) (□), CXCL9(82–103) (○), CXCL9(86–103) (△), CXCL9(1–103) (■), or CXCL9(1–78) (▲)). Bound CXCL8 was detected with biotinylated anti-human CXCL8 antibodies. The mean + S.E. (*error bars*) ($n \geq 4$) percentage inhibition of binding of CXCL8 to heparin of the individual competitors is indicated on the *y* axis. Statistical comparison of the different competitors with CXCL9(74–103) was performed using the Mann-Whitney *U* test (*, $p < 0.05$; **, $p < 0.01$). *B*, CHO/CXCR4 cells were treated with biotinylated CXCL8 in the presence of an excess of CXCL9(74–103) peptide. Bound CXCL8 was detected by streptavidin-allophycocyanin and compared with the amount of bound CXCL8 in the absence of CXCL9(74–103). The percentage of inhibition of CXCL8 binding was calculated and is depicted on the *y* axis. In addition, competition between CXCL11 (*C*) or CCL2 (*D*) and COOH-terminal CXCL9 peptides for binding to heparin or HS, respectively, was performed. *C*, CXCL11 (120, 40, 12, and 4.5 nM) was added to heparin (immobilized in 96-well plates) in the presence/absence of the indicated excess of competitor (CXCL9(74–103) (●), CXCL9(79–103) (□), CXCL9(82–103) (○), CXCL9(86–103) (△), or CXCL9(1–103) (■)). Bound CXCL11 was detected with biotinylated anti-human CXCL11 antibodies. The mean + S.E. ($n \geq 3$) percentage inhibition of binding of CXCL11 to heparin of the individual competitors is indicated on the *y* axis. Statistical comparison of the different competitors with CXCL9(74–103) was performed using the Mann-Whitney *U* test (*, $p < 0.05$; **, $p < 0.01$). *D*, biotinylated CCL2 (500 nM) was added to HS (immobilized in 96-well plates) and incubated with the indicated excess of unlabeled CXCL9(74–103) (●) or CCL2 (♦). Bound biotinylated CCL2 was detected by streptavidin-HRP. The mean + S.E. ($n \geq 3$) percentage inhibition of binding of CCL2 to HS of the individual competitors is indicated on the *y* axis.

cyte subtypes, the infiltrated leukocyte population predominantly consists of neutrophils. The extravasation of these neutrophils is inhibited by 92% by intravenous injection of CXCL9(74–103) and explains the reduced general influx of leukocytes (Fig. 7*B*). Second, the inhibitory activity of the CXCL9(74–103) peptide was evaluated in a model of gout in mice. In this model, injection of MSU crystals induces an inflammasome-dependent production of CXCL1/2 chemokines, which are necessary for CXCR2-mediated recruitment of neutrophils and neutrophil-dependent inflammatory hypernociception (49, 50). As seen in Fig. 7, *C* and *D*, injection of MSU crystals in the knee joint of mice induced significant recruitment of leukocytes, mostly neutrophils. Injection of 100 μg of the CXCL9 peptide intravenously just before the injection of MSU crystals greatly inhibited (87%) leukocyte and neutrophil infiltration in this gout inflammation model. In contrast, the lower doses tested (*i.e.* 10 and 30 μg) were not able to reduce MSU-induced inflammation.

Discussion

Posttranslational modification constitutes an important mechanism of regulating the activity of inflammatory chemokines (27). Frequently, chemokines seem to be subject to NH_2-terminal truncation (28). In contrast, COOH-terminal truncation is only occasionally observed (51–57). The consequences of COOH-terminal truncation are less clear and seem to be rather limited to modification of GAG binding properties (58).

Human myelomonocytic THP-1 cells, stimulated with IFN-γ, were reported to produce CXCL9, which shows a similar pattern of molecular mass protein bands on SDS-PAGE as recombinant CXCL9 produced by CHO cells (59). This recombinant CXCL9 showed COOH-terminal diversity composed of CXCL9(1–103), CXCL9(1–90), CXCL9(1–81), and CXCL9(1–78), as confirmed by mass spectrometry (59). Moreover, incubation of intact CXCL9 with furin, MMP-9, or MMP-7 resulted in the generation of CXCL9(1–101) (furin), CXCL9(1–96)

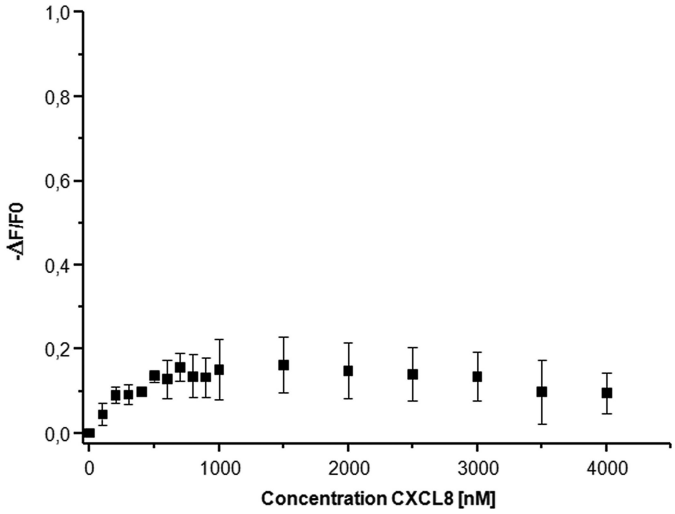

FIGURE 5. **Evaluation of the interaction of CXCL9(74–103) and CXCL8.** Interaction of CXCL9(74–103) and CXCL8 was determined by isothermal fluorescence titration. CXCL8(1–77) was titrated against 600 nM TAMRA-labeled CXCL9(74–103), and the relative change in fluorescence intensity was plotted against the concentration of CXCL8. The mean ± S.E. (*error bars*) ($n = 3$) relative change in fluorescence intensity following ligand addition (ΔF) is calculated as follows: $\Delta F = F$ (fluorescence emission at a certain ligand concentration) $- F_0$ (fluorescence emission in the absence of ligand).

(furin), CXCL9(1–94) (MMP-9), CXCL9(1–93) (MMP-9, furin), CXCL9(1–92) (furin), and CXCL9(1–90) (MMP-9, MMP-7, furin) (56, 58, 60). The biological activity of COOH-terminally truncated CXCL9 was evaluated using synthetic CXCL9(1–73), which showed decreased binding affinity of CXCL9 for CXCR3 by a factor of about 15 (44). Accordingly, CXCL9-induced migration of activated T lymphocytes was reduced upon COOH-terminal truncation.

Upon stimulation with the Th1 cytokine IFN-γ and the TLR3 ligand dsRNA, mimicking an inflammatory situation, both PBMCs and diploid fibroblasts produce substantial amounts of CXCL9 (35). Interestingly, the amount of natural CXCL9 produced by these cells is significantly (10–100-fold) higher than the amount of the 3-fold more potent CXCR3 ligand CXCL11 (data not shown). In the current study, chromatographic purification of the natural human CXCL9 and evaluation of its molecular mass revealed that under the tested inflammatory conditions, all produced CXCL9 was processed COOH-terminally into CXCL9(1–74), CXCL9(1–75), etc. (Table 1). Indeed, under these conditions, natural CXCL9 seems to lose its unique and characteristic COOH-terminal region by which it differs from the other CXCR3 ligands and most other chemokines. The enzymes responsible for the COOH-terminal truncation of CXCL9 in these *in vitro* cell cultures have not been identified. However, plenty of enzymes have been described to COOH-terminally cleave CXCL9 and may be involved in the formation of such isoforms (see above). Because CXCL9(1–73) has been shown to be a less potent T lymphocyte chemoattractant compared with intact CXCL9, these COOH-terminal truncations might be crucial to down-regulate CXCL9 activity in a timely manner. Such posttranslational processing under inflammatory conditions might constitute a negative feedback loop. This COOH-terminal region may either play a role in receptor binding or be important for the cis-presentation of CXCL9 on GAGs to its receptor. In general, GAGs are not an absolute requirement for receptor binding and signaling *in vitro*, but for some chemokines, they have been shown to enhance the sensitivity of a cell to chemokine stimulation (61).

Given the high number of positive charges, one could presume a GAG binding function for the COOH-terminal region of CXCL9. Furthermore, the CXCL9(74–103) peptide was reported not to bind to CXCR3 (44). Keeping this in mind, the following hypothesis was formulated. Do these COOH-terminal CXCL9 peptides, through competition with active chemotactic chemokines for GAG binding, reduce chemokine immobilization and presentation, and do they thereby inhibit chemokine-induced leukocyte migration? Because this region tends to be often removed, it might play a role on its own during an inflammatory reaction. Our data show that the longest of the synthesized peptides (CXCL9(74–103)) clearly interacts with both soluble and cellular GAGs with K_d values in the low nanomolar range. Evaluating heparin binding of the most potent human neutrophil chemoattractant CXCL8 in the presence of the chemically synthesized CXCL9 peptides CXCL9(74–103), CXCL9(79–103), CXCL9(81–103), and CXCL9(86–103) showed that the longest peptide, CXCL9(74–103), clearly reduced CXCL8 binding to heparin, with an efficacy similar to that of intact CXCL9. Furthermore, reducing the length of the COOH-terminal CXCL9 peptide gradually decreased the capacity to compete with CXCL8. These data stress the importance of amino acids 74–78 in the heparin binding characteristics. However, the inability of CXCL9(1–78) to compete with CXCL8 for heparin binding suggests that amino acids 74–78 are necessary but not sufficient for GAG binding. CXCL9(74–103) indeed contains two typical heparin binding motifs (BB*X*B and *X*BBB*XX*B*X*) (Table 1) (*i.e.* Lys^{75}–Lys^{78} and Lys^{85}–Lys^{89}), and both might play an important role in heparin binding of CXCL9.

Competition between CXCL8 and CXCL9(74–103) was also confirmed on cellular GAGs. Furthermore, competition was not limited to CXCL8 and could be extended to CXCL11 and CCL2 (representatives of different chemokine subclasses).

The possibility that CXCL9(74–103) modulates GAG binding properties of CXCL8 through hetero-oligomerization was excluded by both isothermal fluorescence titration and an ELISA-like assay, showing no direct interaction between CXCL9(74–103) and CXCL8. Therefore, the results seen in the GAG binding competition assays can be interpreted as direct competition for GAG binding between CXCL9(74–103) and CXCL8 and should not be the result of chemokine hetero-oligomerization reducing the affinity of CXCL8 for GAGs.

Based on the necessity of chemokine binding to GAGs for exerting biological functions *in vivo*, an anti-inflammatory action for CXCL9(74–103) through GAG binding competition was evaluated in two murine models of acute inflammation, characterized by neutrophil extravasation. In both the CXCL8 model and the less chemokine-specific gout model, intravenous injection of the CXCL9 peptide efficiently inhibited neutrophil-dependent inflammation. The fact that the *in vitro* chemotactic potency of CXCL8 for neutrophils, which is assumed to be based on a GAG-independent soluble chemokine gradient, was not affected by the presence of the CXCL9 peptide confirms the

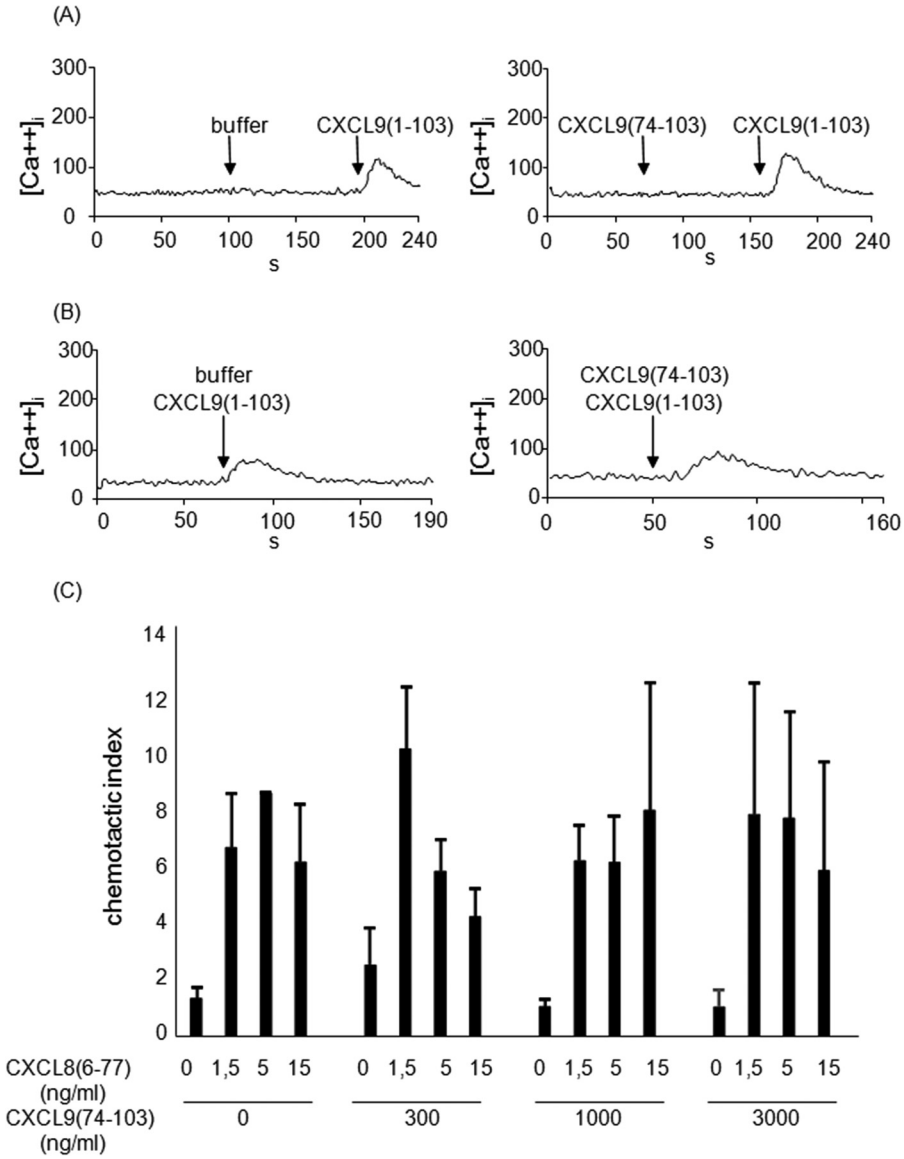

FIGURE 6. **G protein-coupled receptor-dependent activity of CXCL9(74–103).** *A* and *B*, calcium signaling upon stimulation of CXCR3-transfected CHO cells with CXCL9(74–103) and CXCL9(1–103). *A*, the CXCR3-dependent signaling capacity of CXCL9(74–103) was evaluated in CHO cells transfected with human CXCR3 loaded with the ratiometric Ca^{2+}-binding molecule Fura-2. The intracellular Ca^{2+} concentrations ($[Ca^{2+}]_i$ in nM) were calculated from the continuously measured fluorescence intensity ratio of Fura-2 (510 nm) in a LSB50 luminescence spectrophotometer. The cells were stimulated with either 266 ng/ml intact CXCL9 (as a positive control) (*left*) or 1600 ng/ml CXCL9(74–103) (*right*). Potential desensitization of CXCR3 by CXCL9(74–103) was assessed by stimulating the cells with 1600 ng/ml CXCL9(74–103) 100 s prior to stimulation with 266 ng/ml intact CXCL9 (*right*). The response of the cells to stimulation with intact CXCL9 is compared with the response of the cells with prior stimulation with buffer (*left*). *B*, CHO cells transfected with human CXCR3 and loaded with Fura-2 were stimulated with 266 ng/ml CXCL9(1–103) upon prior incubation (10 min) with either buffer (*left*) or 10 μg/ml CXCL9(74–103) (*right*). *C*, the neutrophil chemotactic activity of CXCL8(6–77) in the presence of different concentrations of CXCL9(74–103) was evaluated using 48-well plate Boyden chambers. The mean + S.E. ($n = 8$) chemotactic index, depicted on the *y* axis, is calculated by dividing the amount of migrated cells in response to CXCL8 by the amount of spontaneously migrated cells (in response to buffer). A statistical comparison to evaluate the effect of CXCL9(74–103) was performed using the Mann-Whitney *U* test.

presumption that the inhibitory effect of CXCL9(74–103) is GAG- and not receptor-mediated.

Induction experiments show that the amount of CXCL9 produced by fibroblasts, endothelial cells, and peripheral blood mononuclear cells can clearly exceed the amount of CXCL11, which is active at lower concentrations (35, 62). Therefore, COOH-terminal cleavage might lead to the generation of quite high local concentrations of CXCL9(74–103), which compete with intact functional chemokines for GAG binding. As such, enzymatic cleavage of the COOH-terminal region of CXCL9 might contribute to the resolution of inflammation because it not only directly reduces the activity of CXCL9 but also indirectly, through competition for GAG binding, lowers the activity of other chemokines.

The strength of the peptide *in vivo* might be based on the fact that the peptide is chemokine-derived because it might therefore inherit the chemokine-intrinsic specificity for certain glycosaminoglycan sequences expressed by endothelial cells under inflammatory conditions. The exact composition of the GAGs on endothelial cells and in the extracellular matrix has been shown to depend on the type and location of the cells and the pathophysiological state of the tissue (63, 64). Further *in vivo* investigation is necessary to evaluate the efficacy of the peptide in specific inflammation models (with different GAG profiles)

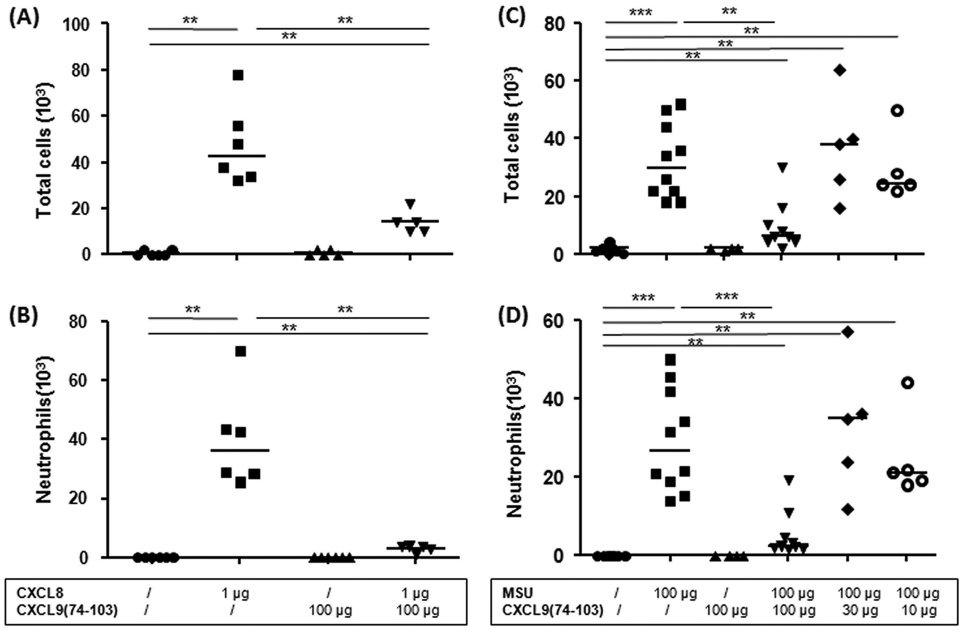

FIGURE 7. **Neutrophil extravasation to the tibiofemoral articulation induced by CXCL8 or MSU crystals in the presence of CXCL9(74–103).** CXCL8(1–77) (*A* and *B*) or MSU crystals (*C* and *D*) were injected into the tibiofemoral articulation of C57BL/6 mice. Simultaneously, CXCL9(74–103) (10, 30, or 100 μg) was injected intravenously. 3 h postinjection, the number of neutrophils present in the cavity was evaluated by washing the cavity and differentially counting the leukocyte subtypes on May-Grunwald-Giemsa-stained cytospins. The total number of leukocytes (*A* and *C*) and neutrophils (*B* and *D*) are shown for every individual mouse, and the *horizontal lines* denote the median number of cells. To detect statistically significant differences, the Mann-Whitney *U* test was carried out (*, $p < 0.05$; **, $p < 0.01$; ***, $p < 0.001$).

to uncover whether it shows a certain specificity for specific pathological conditions.

Although chemokines are clearly beneficial in the battle against infectious organisms and during wound healing after tissue injury, excessive on-going expression of chemokines has been associated with inflammatory disorders, characterized by high levels of leukocyte infiltration (65, 66). Therefore, interfering with the chemokine system might constitute an attractive way of treating such diseases. Interestingly, viruses and ticks have been shown to successfully use this strategy to evade the immune system of the host (67). These organisms encode homologs of chemokines and chemokine receptors or proteins that are able to bind chemokines and thereby control their activity. Therapeutic intervention in the chemokine system has long been focused on the development of chemokine and chemokine receptor antagonists (68). However, the use of these agents in clinical trials, in general, remained unsuccessful. More recently, it has been suggested that interruption of chemokine-GAG interactions might represent an innovative, useful, and effective way of interfering with chemokine action (69). Indeed, in the case of the recently developed CellJammer approach, mutant chemokines are being engineered with increased GAG binding affinity (leaving the specificity unchanged) and abrogated G protein-coupled receptor signaling, creating antagonists for the wild type chemokines through competition for GAG binding. Until now, this approach has been successfully applied to generate antagonists for CXCL8 and CCL2 (43, 70–72). Indeed, CXCL8- and CCL2-based decoy proteins were shown to moderate inflammation in different mouse models (ischemia/reperfusion, renal allograft rejection, antigen-induced arthritis, experimental autoimmune uveitis, MOG_{35-55}-induced chronic experimental autoimmune encephalomyelitis), supporting the potential of this strategy. In view of this, the CXCL9(74–103) might be a lead molecule for the generation of therapeutic peptides that compete with functional chemokines for GAG binding, and its efficacy confirms the applicability of GAGs as a therapeutic target.

Author Contributions—V. V., J. V. D., P. P., and A. M. designed the study. V. V., P. P., and A. M. wrote the paper. All authors analyzed and interpreted the data. V. V., R. J., D. B., N. K., N. B., I. R., F. A. A., P. P., and A. M. performed the experiments. R. J., D. B., F. A. A., and M. M. T. were involved in the mouse inflammation model studies. N. K. and A. J. K. performed isothermal fluorescence titration assays and GAG binding competition assays. V. V., A. M., and P. P. synthesized and purified CXCL9 and performed mass spectrometry and Edman degradation, GAG binding assays, oligomerization studies, and signaling and chemotaxis assays. All authors corrected and approved the final version of the manuscript.

Acknowledgment—We thank Noëmie Pörtner for excellent technical assistance.

References

1. Rot, A., and von Andrian, U. H. (2004) Chemokines in innate and adaptive host defense: basic chemokinese grammar for immune cells. *Annu. Rev. Immunol.* **22,** 891–928
2. Murphy, P. M., Baggiolini, M., Charo, I. F., Hébert, C. A., Horuk, R., Matsushima, K., Miller, L. H., Oppenheim, J. J., and Power, C. A. (2000) International Union of Pharmacology. XXII. Nomenclature for chemokine receptors. *Pharmacol. Rev.* **52,** 145–176
3. Ley, K., Laudanna, C., Cybulsky, M. I., and Nourshargh, S. (2007) Getting to the site of inflammation: the leukocyte adhesion cascade updated. *Nat. Rev. Immunol.* **7,** 678–689
4. Handel, T. M., Johnson, Z., Crown, S. E., Lau, E. K., and Proudfoot, A. E. (2005) Regulation of protein function by glycosaminoglycans: as exempli-

fied by chemokines. *Annu. Rev. Biochem.* **74,** 385–410
5. Johnson, Z., Proudfoot, A. E., and Handel, T. M. (2005) Interaction of chemokines and glycosaminoglycans: a new twist in the regulation of chemokine function with opportunities for therapeutic intervention. *Cytokine Growth Factor Rev.* **16,** 625–636
6. Hileman, R. E., Fromm, J. R., Weiler, J. M., and Linhardt, R. J. (1998) Glycosaminoglycan-protein interactions: definition of consensus sites in glycosaminoglycan binding proteins. *Bioessays* **20,** 156–167
7. Thompson, L. D., Pantoliano, M. W., and Springer, B. A. (1994) Energetic characterization of the basic fibroblast growth factor-heparin interaction: identification of the heparin binding domain. *Biochemistry* **33,** 3831–3840
8. Wang, L., Fuster, M., Sriramarao, P., and Esko, J. D. (2005) Endothelial heparan sulfate deficiency impairs L-selectin- and chemokine-mediated neutrophil trafficking during inflammatory responses. *Nat. Immunol.* **6,** 902–910
9. Proudfoot, A. E., Handel, T. M., Johnson, Z., Lau, E. K., LiWang, P., Clark-Lewis, I., Borlat, F., Wells, T. N., and Kosco-Vilbois, M. H. (2003) Glycosaminoglycan binding and oligomerization are essential for the *in vivo* activity of certain chemokines. *Proc. Natl. Acad. Sci. U.S.A.* **100,** 1885–1890
10. Severin, I. C., Gaudry, J. P., Johnson, Z., Kungl, A., Jansma, A., Gesslbauer, B., Mulloy, B., Power, C., Proudfoot, A. E., and Handel, T. (2010) Characterization of the chemokine CXCL11-heparin interaction suggests two different affinities for glycosaminoglycans. *J. Biol. Chem.* **285,** 17713–17724
11. Campanella, G. S., Grimm, J., Manice, L. A., Colvin, R. A., Medoff, B. D., Wojtkiewicz, G. R., Weissleder, R., and Luster, A. D. (2006) Oligomerization of CXCL10 is necessary for endothelial cell presentation and *in vivo* activity. *J. Immunol.* **177,** 6991–6998
12. Sarris, M., Masson, J. B., Maurin, D., Van der Aa, L. M., Boudinot, P., Lortat-Jacob, H., and Herbomel, P. (2012) Inflammatory chemokines direct and restrict leukocyte migration within live tissues as glycan-bound gradients. *Curr. Biol.* **22,** 2375–2382
13. Massena, S., Christoffersson, G., Hjertström, E., Zcharia, E., Vlodavsky, I., Ausmees, N., Rolny, C., Li, J. P., and Phillipson, M. (2010) A chemotactic gradient sequestered on endothelial heparan sulfate induces directional intraluminal crawling of neutrophils. *Blood* **116,** 1924–1931
14. Bao, X., Moseman, E. A., Saito, H., Petryanik, B., Thiriot, A., Hatakeyama, S., Ito, Y., Kawashima, H., Yamaguchi, Y., Lowe, J. B., von Andrian, U. H., and Fukuda, M. (2010) Endothelial heparan sulfate controls chemokine presentation in recruitment of lymphocytes and dendritic cells to lymph nodes. *Immunity* **33,** 817–829
15. Dyer, D. P., Thomson, J. M., Hermant, A., Jowitt, T. A., Handel, T. M., Proudfoot, A. E., Day, A. J., and Milner, C. M. (2014) TSG-6 inhibits neutrophil migration via direct interaction with the chemokine CXCL8. *J. Immunol.* **192,** 2177–2185
16. Kumar, A. V., Katakam, S. K., Urbanowitz, A. K., and Gotte, M. (2015) Heparan sulphate as a regulator of leukocyte recruitment in inflammation. *Curr. Protein Pept. Sci.* **16,** 77–86
17. Salanga, C. L., and Handel, T. M. (2011) Chemokine oligomerization and interactions with receptors and glycosaminoglycans: the role of structural dynamics in function. *Exp. Cell Res.* **317,** 590–601
18. Middleton, J., Neil, S., Wintle, J., Clark-Lewis, I., Moore, H., Lam, C., Auer, M., Hub, E., and Rot, A. (1997) Transcytosis and surface presentation of IL-8 by venular endothelial cells. *Cell* **91,** 385–395
19. Sadir, R., Imberty, A., Baleux, F., and Lortat-Jacob, H. (2004) Heparan sulfate/heparin oligosaccharides protect stromal cell-derived factor-1 (SDF-1)/CXCL12 against proteolysis induced by CD26/dipeptidyl peptidase IV. *J. Biol. Chem.* **279,** 43854–43860
20. Ellyard, J. I., Simson, L., Bezos, A., Johnston, K., Freeman, C., and Parish, C. R. (2007) Eotaxin selectively binds heparin: an interaction that protects eotaxin from proteolysis and potentiates chemotactic activity *in vivo*. *J. Biol. Chem.* **282,** 15238–15247
21. Weber, M., Hauschild, R., Schwarz, J., Moussion, C., de Vries, I, Legler, D. F., Luther, S. A., Bollenbach, T., and Sixt, M. (2013) Interstitial dendritic cell guidance by haptotactic chemokine gradients. *Science* **339,** 328–332
22. Middleton, J., Patterson, A. M., Gardner, L., Schmutz, C., and Ashton, B. A. (2002) Leukocyte extravasation: chemokine transport and presentation by the endothelium. *Blood* **100,** 3853–3860
23. Kiefer, F., and Siekmann, A. F. (2011) The role of chemokines and their receptors in angiogenesis. *Cell Mol. Life Sci.* **68,** 2811–2830
24. Vandercappellen, J., Van Damme, J., and Struyf, S. (2011) The role of the CXC chemokines platelet factor-4 (CXCL4/PF-4) and its variant (CXCL4L1/PF-4var) in inflammation, angiogenesis and cancer. *Cytokine Growth Factor Rev.* **22,** 1–18
25. Keeley, E. C., Mehrad, B., and Strieter, R. M. (2011) Chemokines as mediators of tumor angiogenesis and neovascularization. *Exp. Cell Res.* **317,** 685–690
26. Mantovani, A., Savino, B., Locati, M., Zammataro, L., Allavena, P., and Bonecchi, R. (2010) The chemokine system in cancer biology and therapy. *Cytokine Growth Factor Rev.* **21,** 27–39
27. Mortier, A., Van Damme, J., and Proost, P. (2012) Overview of the mechanisms regulating chemokine activity and availability. *Immunol. Lett.* **145,** 2–9
28. Mortier, A., Van Damme, J., and Proost, P. (2008) Regulation of chemokine activity by posttranslational modification. *Pharmacol. Ther.* **120,** 197–217
29. Mortier, A., Gouwy, M., Van Damme, J., and Proost, P. (2011) Effect of posttranslational processing on the *in vitro* and *in vivo* activity of chemokines. *Exp. Cell Res.* **317,** 642–654
30. Moelants, E. A., Mortier, A., Van Damme, J., and Proost, P. (2013) *In vivo* regulation of chemokine activity by post-translational modification. *Immunol. Cell Biol.* **91,** 402–407
31. Nibbs, R. J., and Graham, G. J. (2013) Immune regulation by atypical chemokine receptors. *Nat. Rev. Immunol.* **13,** 815–829
32. Schuh, J. M., Blease, K., Kunkel, S. L., and Hogaboam, C. M. (2003) Chemokines and cytokines: axis and allies in asthma and allergy. *Cytokine Growth Factor Rev.* **14,** 503–510
33. Farber, J. M. (1993) HuMig: a new human member of the chemokine family of cytokines. *Biochem. Biophys. Res. Commun.* **192,** 223–230
34. Groom, J. R., and Luster, A. D. (2011) CXCR3 ligands: redundant, collaborative and antagonistic functions. *Immunol. Cell Biol.* **89,** 207–215
35. Proost, P., Verpoest, S., Van de Borne, K., Schutyser, E., Struyf, S., Put, W., Ronsse, I., Grillet, B., Opdenakker, G., and Van Damme, J. (2004) Synergistic induction of CXCL9 and CXCL11 by Toll-like receptor ligands and interferon-γ in fibroblasts correlates with elevated levels of CXCR3 ligands in septic arthritis synovial fluids. *J. Leukoc. Biol.* **75,** 777–784
36. Mortier, A., Berghmans, N., Ronsse, I., Grauwen, K., Stegen, S., Van Damme, J., and Proost, P. (2011) Biological activity of CXCL8 forms generated by alternative cleavage of the signal peptide or by aminopeptidase-mediated truncation. *PLoS One* **6,** e23913
37. Van Raemdonck, K., Berghmans, N., Vanheule, V., Bugatti, A., Proost, P., Opdenakker, G., Presta, M., Van Damme, J., and Struyf, S. (2014) Angiostatic, tumor inflammatory and anti-tumor effects of CXCL447–70 and CXCL4L147–70 in an EGF-dependent breast cancer model. *Oncotarget* **5,** 10916–10933
38. Loos, T., Mortier, A., and Proost, P. (2009) Chapter 1. Isolation, identification, and production of posttranslationally modified chemokines. *Methods Enzymol.* **461,** 3–29
39. Moelants, E. A., Loozen, G., Mortier, A., Martens, E., Opdenakker, G., Mizgalska, D., Szmigielski, B., Potempa, J., Van Damme, J., Teughels, W., and Proost, P. (2014) Citrullination and proteolytic processing of chemokines by *Porphyromonas gingivalis*. *Infect. Immun.* **82,** 2511–2519
40. Gerlza, T., Hecher, B., Jeremic, D., Fuchs, T., Gschwandtner, M., Falsone, A., Gesslbauer, B., and Kungl, A. J. (2014) A combinatorial approach to biophysically characterise chemokine-glycan binding affinities for drug development. *Molecules* **19,** 10618–10634
41. Mortier, A., Loos, T., Gouwy, M., Ronsse, I., Van Damme, J., and Proost, P. (2010) Posttranslational modification of the NH_2-terminal region of CXCL5 by proteases or peptidylarginine deiminases (PAD) differently affects its biological activity. *J. Biol. Chem.* **285,** 29750–29759
42. Gouwy, M., Struyf, S., Noppen, S., Schutyser, E., Springael, J. Y., Parmentier, M., Proost, P., and Van Damme, J. (2008) Synergy between coproduced CC and CXC chemokines in monocyte chemotaxis through receptor-mediated events. *Mol. Pharmacol.* **74,** 485–495
43. Falsone, A., Wabitsch, V., Geretti, E., Potzinger, H., Gerlza, T., Robinson,

J., Adage, T., Teixeira, M. M., and Kungl, A. J. (2013) Designing CXCL8-based decoy proteins with strong anti-inflammatory activity *in vivo*. *Biosci. Rep.* **33,**
44. Clark-Lewis, I., Mattioli, I., Gong, J. H., and Loetscher, P. (2003) Structure-function relationship between the human chemokine receptor CXCR3 and its ligands. *J. Biol. Chem.* **278,** 289–295
45. Struyf, S., Salogni, L., Burdick, M. D., Vandercappellen, J., Gouwy, M., Noppen, S., Proost, P., Opdenakker, G., Parmentier, M., Gerard, C., Sozzani, S., Strieter, R. M., and Van Damme, J. (2011) Angiostatic and chemotactic activities of the CXC chemokine CXCL4L1 (platelet factor-4 variant) are mediated by CXCR3. *Blood* **117,** 480–488
46. Kuschert, G. S., Hoogewerf, A. J., Proudfoot, A. E., Chung, C. W., Cooke, R. M., Hubbard, R. E., Wells, T. N., and Sanderson, P. N. (1998) Identification of a glycosaminoglycan binding surface on human interleukin-8. *Biochemistry* **37,** 11193–11201
47. Nesmelova, I. V., Sham, Y., Dudek, A. Z., van Eijk, L. I., Wu, G., Slungaard, A., Mortari, F., Griffioen, A. W., and Mayo, K. H. (2005) Platelet factor 4 and interleukin-8 CXC chemokine heterodimer formation modulates function at the quaternary structural level. *J. Biol. Chem.* **280,** 4948–4958
48. Feldmann, M., Brennan, F. M., and Maini, R. N. (1996) Role of cytokines in rheumatoid arthritis. *Annu. Rev. Immunol.* **14,** 397–440
49. Martinon, F., Pétrilli, V., Mayor, A., Tardivel, A., and Tschopp, J. (2006) Gout-associated uric acid crystals activate the NALP3 inflammasome. *Nature* **440,** 237–241
50. Amaral, F. A., Costa, V. V., Tavares, L. D., Sachs, D., Coelho, F. M., Fagundes, C. T., Soriani, F. M., Silveira, T. N., Cunha, L. D., Zamboni, D. S., Quesniaux, V., Peres, R. S., Cunha, T. M., Cunha, F. Q., Ryffel, B., Souza, D. G., and Teixeira, M. M. (2012) NLRP3 inflammasome-mediated neutrophil recruitment and hypernociception depend on leukotriene B(4) in a murine model of gout. *Arthritis Rheum.* **64,** 474–484
51. Brandt, E., Petersen, F., and Flad, H. D. (1993) A novel molecular variant of the neutrophil-activating peptide NAP-2 with enhanced biological activity is truncated at the C-terminus: identification by antibodies with defined epitope specificity. *Mol. Immunol.* **30,** 979–991
52. Ehlert, J. E., Petersen, F., Kubbutat, M. H., Gerdes, J., Flad, H. D., and Brandt, E. (1995) Limited and defined truncation at the C terminus enhances receptor binding and degranulation activity of the neutrophil-activating peptide 2 (NAP-2): comparison of native and recombinant NAP-2 variants. *J. Biol. Chem.* **270,** 6338–6344
53. Ehlert, J. E., Gerdes, J., Flad, H. D., and Brandt, E. (1998) Novel C-terminally truncated isoforms of the CXC chemokine β-thromboglobulin and their impact on neutrophil functions. *J. Immunol.* **161,** 4975–4982
54. Krijgsveld, J., Zaat, S. A., Meeldijk, J., van Veelen, P. A., Fang, G., Poolman, B., Brandt, E., Ehlert, J. E., Kuijpers, A. J., Engbers, G. H., Feijen, J., and Dankert, J. (2000) Thrombocidins, microbicidal proteins from human blood platelets, are C-terminal deletion products of CXC chemokines. *J. Biol. Chem.* **275,** 20374–20381
55. Hensbergen, P. J., van der Raaij-Helmer, E. M., Dijkman, R., van der Schors, R. C., Werner-Felmayer, G., Boorsma, D. M., Scheper, R. J., Willemze, R., and Tensen, C. P. (2001) Processing of natural and recombinant CXCR3-targeting chemokines and implications for biological activity. *Eur. J. Biochem.* **268,** 4992–4999
56. Hensbergen, P. J., Verzijl, D., Balog, C. I., Dijkman, R., van der Schors, R. C., van der Raaij-Helmer EM, van der Plas, M. J., Leurs, R., Deelder, A. M., Smit, M. J., and Tensen, C. P. (2004) Furin is a chemokine-modifying enzyme: *in vitro* and *in vivo* processing of CXCL10 generates a C-terminally truncated chemokine retaining full activity. *J. Biol. Chem.* **279,** 13402–13411
57. Denis, C., Deiteren, K., Mortier, A., Tounsi, A., Fransen, E., Proost, P., Renauld, J. C., and Lambeir, A. M. (2012) C-terminal clipping of chemokine CCL1/I-309 enhances CCR8-mediated intracellular calcium release and anti-apoptotic activity. *PLoS One* **7,** e34199
58. Cox, J. H., Dean, R. A., Roberts, C. R., and Overall, C. M. (2008) Matrix metalloproteinase processing of CXCL11/I-TAC results in loss of chemoattractant activity and altered glycosaminoglycan binding. *J. Biol. Chem.* **283,** 19389–19399
59. Liao, F., Rabin, R. L., Yannelli, J. R., Koniaris, L. G., Vanguri, P., and Farber, J. M. (1995) Human Mig chemokine: biochemical and functional characterization. *J. Exp. Med.* **182,** 1301–1314
60. Van den Steen, P. E., Husson, S. J., Proost, P., Van Damme, J., and Opdenakker, G. (2003) Carboxyterminal cleavage of the chemokines MIG and IP-10 by gelatinase B and neutrophil collagenase. *Biochem. Biophys. Res. Commun.* **310,** 889–896
61. Ali, S., Palmer, A. C., Banerjee, B., Fritchley, S. J., and Kirby, J. A. (2000) Examination of the function of RANTES, MIP-1α, and MIP-1β following interaction with heparin-like glycosaminoglycans. *J. Biol. Chem.* **275,** 11721–11727
62. Loos, T., Dekeyzer, L., Struyf, S., Schutyser, E., Gijsbers, K., Gouwy, M., Fraeyman, A., Put, W., Ronsse, I., Grillet, B., Opdenakker, G., Van Damme, J., and Proost, P. (2006) TLR ligands and cytokines induce CXCR3 ligands in endothelial cells: enhanced CXCL9 in autoimmune arthritis. *Lab. Invest.* **86,** 902–916
63. Selvan, R. S., Ihrcke, N. S., and Platt, J. L. (1996) Heparan sulfate in immune responses. *Ann. N.Y. Acad. Sci.* **797,** 127–139
64. Blackhall, F. H., Merry, C. L., Davies, E. J., and Jayson, G. C. (2001) Heparan sulfate proteoglycans and cancer. *Br. J. Cancer* **85,** 1094–1098
65. Proost, P., Struyf, S., Loos, T., Gouwy, M., Schutyser, E., Conings, R., Ronsse, I., Parmentier, M., Grillet, B., Opdenakker, G., Balzarini, J., and Van Damme, J. (2006) Coexpression and interaction of CXCL10 and CD26 in mesenchymal cells by synergising inflammatory cytokines: CXCL8 and CXCL10 are discriminative markers for autoimmune arthropathies. *Arthritis Res. Ther.* **8,** R107
66. Szekanecz, Z., Vegvari, A., Szabo, Z., and Koch, A. E. (2010) Chemokines and chemokine receptors in arthritis. *Front. Biosci. (Schol. Ed.)* **2,** 153–167
67. Alcami, A., and Lira, S. A. (2010) Modulation of chemokine activity by viruses. *Curr. Opin. Immunol.* **22,** 482–487
68. Allegretti, M., Cesta, M. C., Garin, A., and Proudfoot, A. E. (2012) Current status of chemokine receptor inhibitors in development. *Immunol. Lett.* **145,** 68–78
69. Adage, T., Piccinini, A. M., Falsone, A., Trinker, M., Robinson, J., Gesslbauer, B., and Kungl, A. J. (2012) Structure-based design of decoy chemokines as a way to explore the pharmacological potential of glycosaminoglycans. *Br. J. Pharmacol.* **167,** 1195–1205
70. Liehn, E. A., Piccinini, A. M., Koenen, R. R., Soehnlein, O., Adage, T., Fatu, R., Curaj, A., Popescu, A., Zernecke, A., Kungl, A. J., and Weber, C. (2010) A new monocyte chemotactic protein-1/chemokine CC motif ligand-2 competitor limiting neointima formation and myocardial ischemia/reperfusion injury in mice. *J. Am. Coll. Cardiol.* **56,** 1847–1857
71. Bedke, J., Nelson, P. J., Kiss, E., Muenchmeier, N., Rek, A., Behnes, C. L., Gretz, N., Kungl, A. J., and Gröne, H. J. (2010) A novel CXCL8 protein-based antagonist in acute experimental renal allograft damage. *Mol. Immunol.* **47,** 1047–1057
72. Piccinini, A. M., Knebl, K., Rek, A., Wildner, G., Diedrichs-Möhring, M., and Kungl, A. J. (2010) Rationally evolving MCP-1/CCL2 into a decoy protein with potent anti-inflammatory activity in vivo. *J. Biol. Chem.* **285,** 8782–8792